Self-Assembly with Postmodification: Kinetically Stabilized Metalla-Supramolecular Rectangles

Christopher J. Kuehl,* Songping D. Huang,† and Peter J. Stang*

Contribution from the Departments of Chemistry, University of Utah, Salt Lake City, Utah 84112, and Kent State University, Kent, Ohio 44242

Received June 11, 2001

Abstract: Interaction of a predesigned molecular "clip" (**4**) with rigid dipyridyl bridging ligands, in acetone/water mixtures, leads to the formation of molecular rectangles (**5**−**8**) in 92−97% isolated yields via spontaneous self-assembly. Characterization was accomplished with multinuclear NMR and UV−vis spectroscopy, FAB mass spectrometry, and X-ray crystallography. The length of these metallamacrocycles ranges from 2 to 3 nm. Postmodification via non-nucleophilic counterion exchange results in enhanced structural integrity for the assemblies.

Introduction

Over the past decade, the use of metal coordination as a means to drive and preserve the formation of discrete molecular ensembles has become an established methodology in supramolecular chemistry.[1] However, the level of complexity to which metal-mediated self-assembly can develop as a general synthetic strategy has yet to be realized. The design and construction of new supramolecular entities refine our understanding of the fundamental principles of molecular self-organization.

So far, highly symmetric ring systems (e.g., molecular triangles, squares, pentagons, hexagons, etc.) have generally been the most successfully characterized species, because of their inherent simplicity over three-dimensional constructs. Typically comprising aromatic bridging ligands connected through transition metals, these metallacyclophanes have shown promise as a new class of functional receptor molecules. Because of their charges, these cationic complexes are thought to be ideal for the uptake of anions. In certain cases, anions serve as templates for macrocycle assembly.[2] Developing new paradigms for selective anion sensing is a topic of considerable current interest.[3] A few studies demonstrated molecular squares to be capable of acting as hosts for small aromatic molecules in both aqueous[4] and nonpolar media.[5] When considering that metal-containing macrocycles often possess magnetic, photophysical, and/or redox properties not accessible from purely organic systems, such studies in basic host−guest chemistry have broad implications for technologies such as molecular sensing,[6] separations, and catalysis.[7] However, because of the precise size and the highly specific electrostatic and dispersion forces that are required, selectivity by and large remains an issue.[8]

† Kent State University.

(1) (a) Leininger, S.; Olenyuk, B.; Stang, P. J. *Chem. Rev.* **2000**, *100*, 853. (b) Swiegers, G. F.; Malefetse, T. J. *Chem. Rev.* **2000**, *100*, 3483. (c) Caulder, D. L.; Raymond, K. N. *J. Chem. Soc., Dalton Trans.* **1999**, *8*, 1185. (d) Caulder, D. L.; Raymond, K. N. *Acc. Chem. Res.* **1999**, *32* (11), 975. (e) Chambron, J.-C.; Dietrich-Buchecker, C.; Sauvage, J.-P. Transition Metals as Assembling and Templating Species. In *Comprehensive Supramolecular Chemistry*; Lehn, J.-M., Chair, E., Atwood, J. L., Davis, J. E. D., MacNicol, D. D., Vögtle, F., Eds.; Permagon Press: Oxford, 1996; Vol. 9, Chapter 2, p 43. (f) Baxter, P. N. W. Metal Ion Directed Assembly of Complex Molecular Architectures and Nanostructures. In *Comprehensive Supramolecular Chemistry*; Lehn, J.-M., Chair, E., Atwood, J. L., Davis, J. E. D., MacNicol, D. D., Vögtle, F., Eds.; Permagon Press: Oxford, 1996; Vol. 9, Chapter 5, p 165. (g) Fujita, M. *Chem. Soc. Rev.* **1998**, *6*, 417. (h) Uller, E.; Demleitner, I.; Bernt, I.; Saalfrank, R. W. Synergistic Effect of Serendipity and Rational Design in Supramolecular Chemistry. In *Structure and Bonding*; Fujita, M., Ed.; Springer: Berlin, 2000; Vol. 96, p 149. (i) Baxter, P. N. W.; Lehn, J.-M.; Baum, G.; Fenske, D. *Chem. Eur. J.* **1999**, *5*, 102.

(2) (a) Campos-Fernández, C. S.; Clérac, R.; Koomen, J. M.; Russell, D. H.; Dunbar, K. R. *J. Am. Chem. Soc.* **2001**, *123*, 773. (b) Campos-Fernández, C. S.; Clérac, R.; Dunbar, K. R. *Angew. Chem., Int. Ed. Engl.* **1999**, *38*, 3477. (c) Schnebeck, R.-D.; Freisinger, E.; Lippert, B. *Angew. Chem., Int. Ed. Engl.* **1999**, *38*, 168. (d) McMorran, D. A.; Steel, P. J. *Angew. Chem., Int. Ed. Engl.* **1998**, *37*, 3295. (d) Hasenknopf, B.; Lehn, J.-M.; Boumediene, N.; Leize, E.; Van Dorsselaer, A. *Angew. Chem., Int. Ed. Engl.* **1998**, *37*, 3265. (e) Fleming, J. S.; Mann, K. L. V.; Carraz, C.-A.; Psillakis, E.; Jeffrey, J. C.; McCleverty, J. A.; Ward, M. D. *Angew. Chem., Int. Ed. Engl.* **1998**, *37*, 1279. (f) Vilar, R.; Mingos, D. M. P.; White, A. J. P.; Williams, D. J. *Angew. Chem., Int. Ed. Engl.* **1998**, *37*, 1258. (g) Jones, P. L.; Byrom, K. J.; Jeffrey, J. C.; McCleverty, J. A.; Ward, M. D. *Chem. Commun.* **1997**, 1361. (h) Hasenknopf, B.; Lehn, J.-M.; Boumediene, N.; Dupont-Gervais, A.; Van Dorsselaer, A.; Kniesel, B.; Fenske, D. *J. Am. Chem. Soc.* **1997**, *119*, 10956. (i) Mann, S.; Huttner, G.; Zsolnai, L.; Heinze, K. *Angew. Chem., Int. Ed. Engl.* **1996**, *35*, 2808. (j) Hasenknopf, B.; Lehn, J.-M.; Kniesel, B. O.; Baum, G.; Fenske, D. *Angew. Chem., Int. Ed. Engl.* **1996**, *35*, 1838.

(3) (a) Beer, P. D.; Gale, P. A. *Angew. Chem., Int. Ed. Engl.* **2001**, *40*, 486. (b) Schmidten, F. P.; Berger, M. *Chem. Rev.* **1997**, *97*, 1609. (c) Beer, P. D.; Smith, D. K. *Prog. Inorg. Chem.* **1997**, *46*, 1. (d) Katz, H. E. In *Inclusion Compounds*; Atwood, J. L., Davies, J. E. D., MacNicol, D. D., Eds.; Oxford University Press: New York, 1991; Vol. 4, Chapter 9. (e) Antonise, M. M. G.; Reinhoudt, D. N. *Chem. Commun.* **1998**, 443.

(4) (a) Fujita, M.; Sasaki, O.; Mitsuhashi, T.; Fujita, T.; Yazaki, J.; Yamaguchi, K.; Ogura, K. *J. Chem. Soc., Chem. Commun.* **1996**, 1535. (b) Lee, S. B.; Hwang, S.; Chung, D. S.; Yun, H.; Hong, J.-I. *Tetrahedron Lett.* **1998**, *39*, 873.

(5) (a) Cho, Y. L.; Uh, H.; Chang, S.-Y.; Chang, H.-Y.; Choi, M.-G.; Shin, I.; Jeong, K.-S. *J. Am. Chem. Soc.* **2001**, *123*, 1258. (b) Stang, P. J.; Cao, D. H.; Saito, S.; Arif, A. M. *J. Am. Chem. Soc.* **1995**, *117*, 6273. (c) Whiteford, J. A.; Stang, P. J.; Huang, S. D. *Inorg. Chem.* **1998**, *37*, 5595. (d) Benkstein, K. D.; Hupp, J. T.; Stern, C. L. *J. Am. Chem. Soc.* **1998**, *120*, 12982.

(6) (a) Keefe, M. H.; Benkstein, K. D.; Hupp, J. T. *Coord. Chem. Rev.* **2000**, *205*, 201. (b) Chang, S. H.; Chung, K. B.; Slone, R. V.; Hupp, J. T. *Synth. Met.* **2001**, *117*, 215. (c) Keefe, M. H.; Slone, R. V.; Hupp, J. T.; Czaplewski, K. F.; Snurr, R. Q.; Stern, C. L. *Langmuir* **2000**, *16*, 3964. (d) Benkstein, K. D.; Hupp, J. T. *Mol. Cryst. Liq. Cryst.* **2000**, *342*, 151. (e) Sun, S.-S.; Lees, A. J. *J. Am. Chem. Soc.* **2000**, *122*, 8956. (f) Bélanger, S.; Hupp, J. T. *Angew. Chem., Int. Ed. Engl.* **1999**, *38*, 2222. (g) Bélanger, S.; Hupp, J. T.; Stern, C. L.; Slone, R. V.; Watson, D. F.; Carrell, T. G. *J. Am. Chem. Soc.* **1999**, *121*, 557.

(7) (a) Kang, J.; Rebek, J., Jr. *Nature* **1997**, *385*, 50. (b) Fujita, M.; Kwon, Y. J.; Washizu, S.; Ogura, K. *J. Am. Chem. Soc.* **1994**, *116*, 1151.

10.1021/ja0114355 CCC: $20.00
Published on Web 09/05/2001

Scheme 1

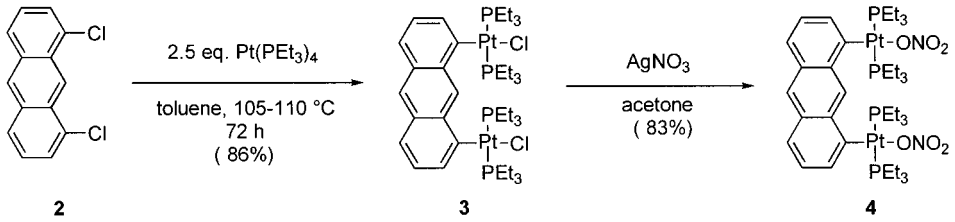

As lower symmetry hosts can ultimately be expected to show enhanced selectivity, especially toward planar aromatic guests, rectangles represent a natural progression in the development of this area. Despite their relative simplicity, molecular rectangles[9] have remained rather uncommon in comparison with the various higher-symmetry polygons (especially molecular squares) that have been prepared and studied. A rational basis for this dearth is that mixed ligand species[10] have rarely been observed; that is, the combination of metals with different length ligands usually leads to complexes containing only one type of ligand. For example, Hupp[11] has shown that reaction of two equivalents of $Re(CO)_5Cl$ with one equivalent each of pyrazine and 4,4′-dipyridyl exclusively gave two separate square assemblies, despite the statistical possibility of forming at least 50% rectangle. Both Lehn[12] and Raymond[13] have undertaken similar studies showing the same type of preferences using helicates. Hence, the difficulty in the construction of rectangular architectures lies in the necessity of designing a building unit with two parallel coordination sites facing in the same direction.

We report herein the design and self-assembly of a series of molecular rectangles via a new type of modular subunit termed a molecular "clip" (**4**). The structure and properties of these nanoscopic, macrocyclic species have been studied by X-ray crystallography, FAB-mass spectrometry, NMR, and UV−vis spectroscopy. Furthermore, the effect that solvent and counterion have on the thermodynamic and kinetic stability of the assemblies, respectively, is described.

Results and Discussion

Design and Synthesis of the Molecular "Clip" (4). Early attempts at preparing molecular rectangles were carried out using the 4,4′-*cis*-platinum-functionalized biphenyl **1**. However, reaction of this subunit with linear dipyridyl ligands such as 4,4′-dipyridyl resulted in the rapid precipitation of a polymeric material, presumably because of the internal rotational freedom available to **1**.[14] It thus appeared that a more rigid subunit was required.

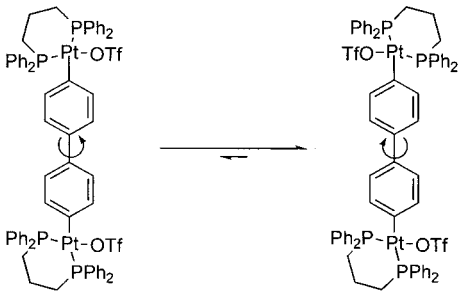

1,8-Dichloroanthracene (**2**),[15] easily prepared by reduction of the commercially available 1,8-dichloroanthraquinone, offers the feasibility of rigidly directing functionality in a parallel fashion, that is, a *ligand-directed* design. Attaching the appropriate desired functionality was achieved by a double oxidative addition strategy.[16] Reaction of 2.5 equiv of $Pt(PEt_3)_4$ with **2** in refluxing toluene generated the dimetallic species **3** in high yield (Scheme 1). Subsequent reaction with silver triflate resulted in decomposition. However, chloride abstraction with silver nitrate in acetone furnished a stable system, **4**, that was found to be neither oxygen nor moisture sensitive. 1,8-Bis(*trans*-$Pt(PEt_3)_2(NO_3)$)anthracene (**4**) was recrystallized from boiling methanol to give a yellow, microcrystalline solid in an overall isolated yield of 71%. Complex **4** was found to be highly soluble in most chlorinated solvents, as well as in nitromethane and acetonitrile, insoluble in hexanes, and partially soluble in acetone, ether, and alcohols. The characterization of **4** was accomplished by NMR spectroscopy (^1H, $^{13}C\{^1H\}$, $^{31}P\{^1H\}$) and elemental analysis and is outlined in the Experimental Section. In addition, crystals of **4**, grown by allowing a CH_2Cl_2/MeOH solution of the complex to slowly evaporate, were analyzed by X-ray diffraction (Table 1). Depicted as an ORTEP representation in the top of Figure 1, the most significant feature in the structure of **4** is that adjacent triethylphosphine ligands are sterically crowded: a likely explanation for the excess (2.5 equiv) of $Pt(PEt_3)_4$ and the longer reaction time required for the conversion of **2** to **3**. As a result, the ligand geometry has slightly deviated from planarity toward a tetrahedral configuration, approximately 13° as defined by the dihedral angle between the P(1)−Pt(1)−C(1) and P(2)−Pt(1)−O(1) planes, for example. Selected bond distances and angles are collected in Table 2. As more clearly evidenced by the CPK representation (bottom

(8) *Inclusion Phenomenon and Molecular Recognition*; Atwood, J. L., Ed. Plenum Press: New York, 1990.

(9) (a) Sommer, R. D.; Rheingold, A. L.; Goshe, A. J.; Bosnich, B. *J. Am. Chem. Soc.* **2001**, *123*, 3940. (b) Manimaran, B.; Rajendran, T.; Lu, Y.-L.; Lee, G.-H.; Peng, S.-M.; Lu, K.-L. *J. Chem. Soc., Dalton Trans.* **2001**, 515. (c) Kuehl, C. J.; Mayne, C. L.; Arif, A. M.; Stang, P. J. *Org. Lett.* **2000**, *2*, 3727. (d) Suzuki, H.; Tajima, N.; Tatsumi, K.; Yamamoto, Y. *Chem. Commun.* **2000**, 1801. (e) Rajendran, T.; Manimaran, B.; Lee, F.-Y.; Lee, G.-H.; Peng, S.-M.; Wang, C. M.; Lu, K.-L. *Inorg. Chem.* **2000**, *39*, 2016. (f) Yan, H.; Süss-Fink, G.; Neels, A.; Stoeckli-Evans, H. *J. Chem. Soc., Dalton Trans.* **1997**, 4345. (g) Benkstein, K. D.; Hupp, J. T.; Stern, C. L. *Inorg. Chem.* **1998**, *37*, 5404. (h) Woessner, S. M.; Helms, J. B.; Shen, Y.; Sullivan, B. P. *Inorg. Chem.* **1998**, *37*, 5407. (i) Benkstein, K. D.; Hupp, J. T.; Stern, C. L. *Angew. Chem., Int. Ed. Engl.* **2000**, *39*, 2891. (j) Holliday, B. J.; Mirkin, C. A. *Angew. Chem., Int. Ed.* **2001**, *40*, 2022.

(10) (a) Baxter, P. N.; Lehn, J.-M.; DeCian, A. *Angew. Chem., Int. Ed. Engl.* **1993**, *32*, 69. (b) Hasenknopf, B.; Lehn, J.-M.; Baum, G.; Fenske, D. *Proc. Natl. Acad. Sci.* **1996**, *93*, 1397. (c) Baxter, P. N.; Lehn, J.-M.; Kneisel, B. O.; Fenske, D. *Angew. Chem., Int. Ed. Engl.* **1997**, *36*, 1978.

(11) Slone, R. V.; Benkstein, K. D.; Bélanger, S.; Hupp, J. T.; Guzei, I. A.; Rheingold, A. L. *Coord. Chem. Rev.* **1998**, *171*, 221.

(12) Kramer, R.; Lehn, J.-M.; Marquis-Rigult, A. *Proc. Natl. Acad. Sci.* **1993**, *90*, 5394.

(13) Caulder, D. L.; Raymond, K. N. *Angew. Chem., Int. Ed. Engl.* **1997**, *36*, 1440.

(14) Olenyuk, B. O.; Stang, P. J. Unpublished results.

(15) House, H. O.; Hrabie, J. A.; VanDerveer, D. *J. Org. Chem.* **1986**, *51*, 921.

(16) Manna, J.; Kuehl, C. J.; Whiteford, J. A.; Stang, P. J. *Organometallics* **1997**, *16*, 1897.

Table 1. Crystallographic Data for **4**, **7**, and **8**

	4	**7**	**8**
empirical formula	$C_{38}H_{68}N_2O_6P_4Pt_2$	$C_{116}H_{160}Cl_4N_4O_{16}P_8Pt_4$	$C_{112}H_{156}F_{24}N_4O_2P_{12}Pt_4$
fw	1163.00	3036.52	3198.50
T (K)	293(2)	173(2)	173(2)
wavelength (Å)	0.710 73	0.710 73	0.710 73
cryst syst	triclinic	triclinic	monoclinic
space group	$P\bar{1}$ (No. 2)	$P\bar{1}$ (No. 2)	$C2/m$ (No. 12)
unit cell dimensions	a = 11.9280(4) Å, α = 80.497(2)° b = 13.5746(5) Å, β = 89.541(2)° c = 15.8310(5) Å, γ = 65.335(2)°	a = 10.0857(3) Å, α = 103.367(1)° b = 15.3995(4) Å, β = 97.202(1)° c = 24.6823(7) Å, γ = 93.207(1)°	a = 20.6877(7) Å, α = 90° b = 39.9232(14) Å, β = 103.702(2)° c = 21.3681(7) Å, γ = 90°
V (Å^3)	2292.2(1)	3685.9(2)	17 146.1(8)
Z	2	1	4
density (Mg/m^3, calcd)	1.685	1.331	1.194
abs coeff (mm^{-1})	6.278	3.957	3.420
θ range for data collection	3.11−32.53°	1.36−28.21°	1.42−28.28°
final R indices [I > 2σ(I)][a]	R1 = 0.057, wR2 = 0.132	R1 = 0.081, wR = 0.215	R1 = 0.079, wR = 0.245
R indices (all data)	R1 = 0.108, wR2 = 0.158	R1 = 0.186, wR2 = 0.267	R1 = 0.156, wR2 = 0.308

[a] $wR2 = \{\sum[w(F_o^2 - F_c^2)^2]/\sum[w(F_o^2)^2]\}^{1/2}$; $R1 = \sum||F_o| - |F_c||/\sum|F_o|$.

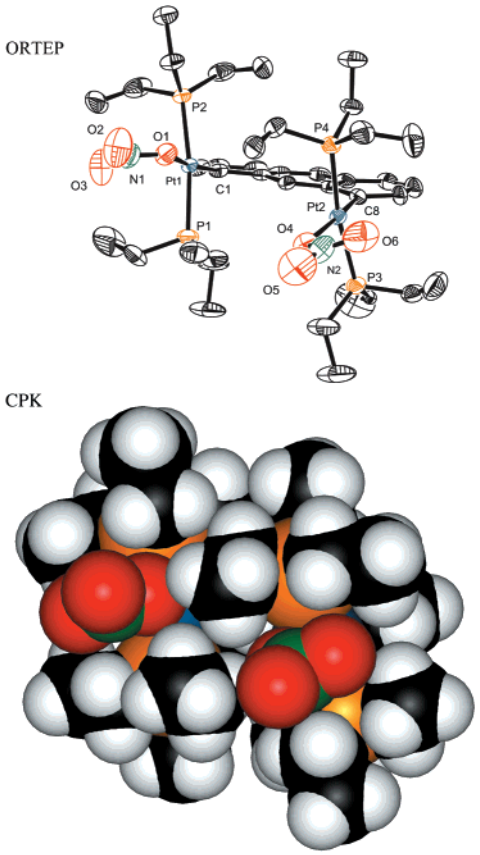

Figure 1. Top: ORTEP diagram of **4** with hydrogens omitted for clarity. Thermal ellipsoids are drawn to 30% probability. Bottom: Space filling representation of **4** (hydrogens included).

of Figure 1), it appears that this repulsion has been partially relieved by the entire molecule adopting a slight dihedral twist ($\phi \cong 15°$). We speculate that these distortions are the reason that the analogous triflate salt is unstable; a few studies have suggested that bent geometries around square planar d^8 complexes can alter reactivity at the metal center.[17] Though slightly distorted, **4** possesses the necessary two labile coordination sites locked into a parallel arrangement, that is, a molecular "clip."

Self-Assembly and Characterization of Nanoscopic Molecular Rectangles. The preparation of several discrete nanoscopic rectangular complexes can be achieved with simplicity and, given the proper conditions, in essentially quantitative yield. The assembly of these macrocycles is most easily monitored

Table 2. Selected Bond Lengths (Å) and Angles (°) for **4**

Bond Lengths			
Pt(1)−C(1)	2.001(8)	Pt(2)−C(8)	1.990(7)
Pt(1)−P(1)	2.306(2)	Pt(2)−P(3)	2.323(2)
Pt(1)−P(2)	2.3188(19)	Pt(2)−P(4)	2.309(2)
Pt(1)−O(1)	2.175(7)	Pt(2)−O(4)	2.154(6)
Bond Angles			
C(1)−Pt(1)−O(1)	169.7(3)	C(8)−Pt(2)−O(4)	170.6(3)
C(1)−Pt(1)−P(1)	90.7(2)	C(8)−Pt(2)−P(4)	90.0(2)
O(1)−Pt(1)−P(1)	93.35(19)	O(4)−Pt(2)−P(4)	94.23(18)
C(1)−Pt(1)−P(2)	88.9(2)	C(8)−Pt(2)−P(3)	89.3(2)
O1−Pt(1)−P(2)	88.57(18)	O(4)−Pt(2)−P(3)	87.85(18)
P(1)−Pt(1)−P(2)	171.20(9)	P(4)−Pt(2)−P(3)	170.64(9)

by examination of their ^{1}H and ^{31}P{^{1}H} NMR spectra. For example, when **4** is combined with an equimolar amount of 4,4′-dipyridyl in a 1:1 (v:v) acetone-d_6/D_2O mixture (Scheme 2), a pale yellow suspension results, which, upon gentle heating, gradually dissolves to give a bright orange homogeneous solution of the smallest rectangle described in this paper, structural motif **5**.[9c] ^{31}P{^{1}H} NMR (121.4 MHz) analysis of the reaction solution is consistent with the formation of a single, highly symmetrical species by the appearance of a sharp singlet with concomitant ^{195}Pt satellites, shifted 6.0 ppm upfield ($\Delta\delta$) relative to **4** ($\Delta^1J_{PPt} = -208$ ppm). In a similar manner, reaction of molecular "clip" **4** with bridging ligands *trans*-1,2-bis(4-pyridyl)ethylene (BPE), 1,4-bis(4′-pyridylethynyl)benzene (BPEB),[18] and 2,5-bis(4′-pyridylethynyl)furan (BPEF)[19] yielded

(17) (a) Romeo, R.; Fenech, L.; Scolaro, L. M.; Albinati, A.; Macchioni, A.; Zuccaccia, C. *Inorg. Chem.* **2001**, *40*, 3293. (b) Fanizzi, F. P.; Intini, F. P.; Maresca, L.; Natile, G.; Lanfranchi, M.; Tiripicchio, A. *J. Chem. Soc., Dalton Trans.* **1991**, 1007. (c) Albano, V. G.; Ferrara, M. L.; Monari, M.; Panunzi, A.; Ruffo, F. *Inorg. Chim. Acta* **1999**, *285*, 70. (d) De Felice, V.; Ferrara, M. L.; Giordano, F.; Ruffo, F. *Gazz. Chim. Ital.* **1994**, *124*, 117. (e) Giordano, F.; Ruffo, F.; Saporito, A.; Panunzi, A. *Inorg. Chim. Acta* **1997**, *264*, 231. (f) Fanizzi, F. P.; Natile, G.; Lanfranchi, M.; Tiripicchio, A.; Pacchioni, G. *Inorg. Chim. Acta* **1998**, *275*, 500. (g) Albano, V. G.; Castellari, C.; Monari, M.; De Felice, V.; Panunzi, A.; Ruffo, F. *Organometallics* **1996**, *15*, 4012. (h) Albano, V. G.; Castellari, C.; Monari, M.; De Felice, V.; Panunzi, A.; Ruffo, F. *Organometallics* **1992**, *11*, 3665. (i) Romeo, R.; Monsù Scolaro, L.; Nastasi, N.; Arena, G. *Inorg. Chem.* **1996**, *35*, 5087. (j) Fanizzi, F. P.; Lanfranchi, M.; Natile, G.; Tiripicchio, A. *Inorg. Chem.* **1994**, *33*, 3331. (k) Clark, H. C.; Hampden-Smith, M. J. *Coord. Chem. Rev.* **1987**, *79*, 229. (l) Skibsted, L. H. *Adv. Inorg. Bioinorg. Mech.* **1986**, *4*, 137. (m) Jones, R. A.; Real, F. M.; Wilkinson, G.; Gulos, A. N. R.; Hursthouse, M. B.; Malik, K. M. A. *J. Chem. Soc., Dalton Trans.* **1980**, 511. (n) Bandyopadhyay, D.; Bandyopadhyay, P.; Chakravorty, A.; Cotton, F. A.; Falvello, L. R. *Inorg. Chem.* **1984**, *23*, 1785. (o) Minghetti, G.; Cinellu, M. A.; Chelucci, G.; Gladiali, S. *J. Organomet. Chem.* **1986**, *307*, 107.

(18) Champness, N. R.; Khlobystov, A. N.; Majuga, A. G.; Schroeder, M.; Zyk, N. V. *Tetrahedron Lett.* **1999**, *40*, 5413.

Scheme 2

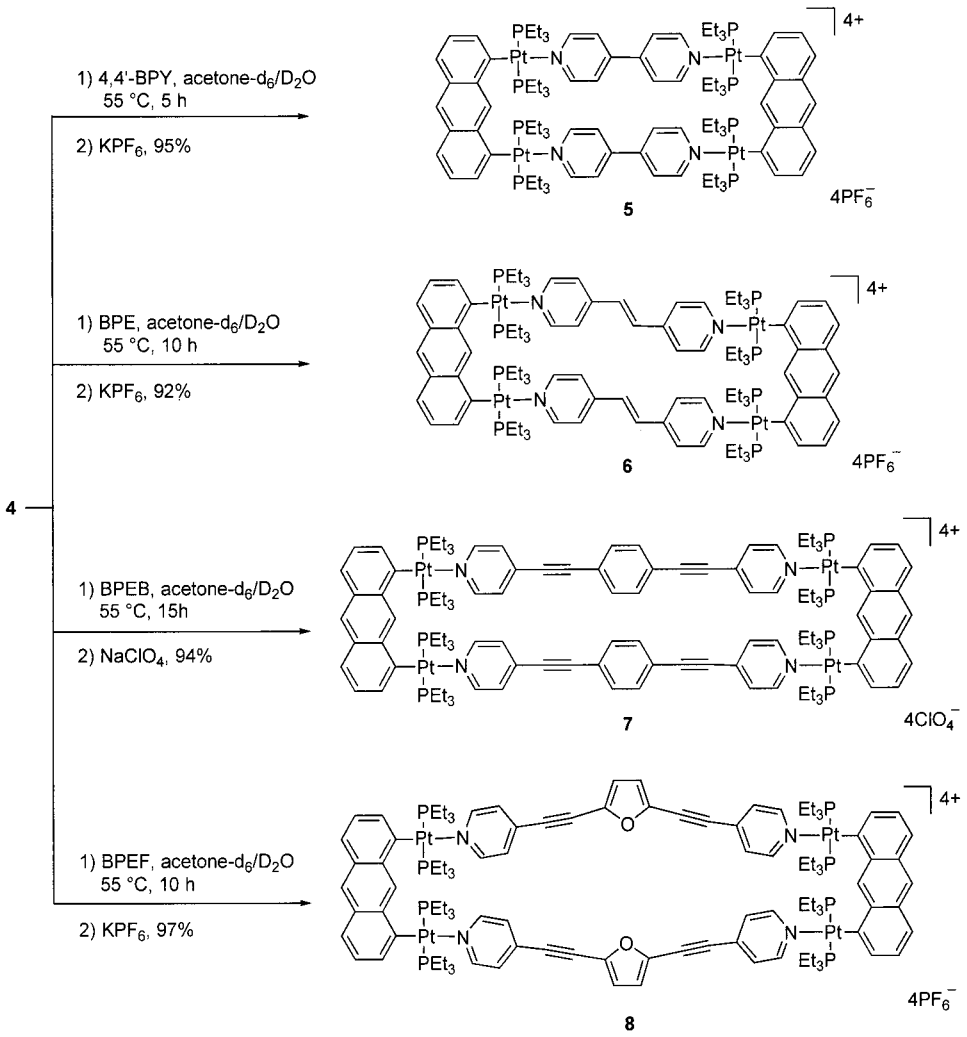

the molecular rectangles **6**, **7**, and **8**, respectively, of differing topology and dimensions (Scheme 2).

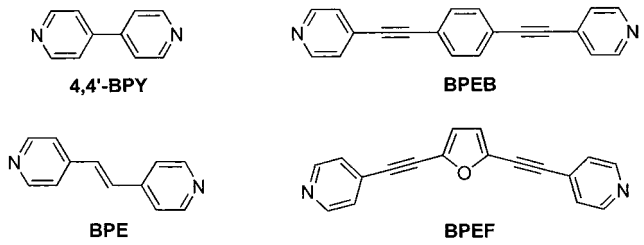

Examination of the ^{1}H NMR (300 MHz) spectra of macrocycles **5**−**8** was also indicative of highly symmetrical structures and displayed significant spectroscopic differences from their monomeric subunits. While the chemical shifts of the protons of the ancillary PEt_3 ligands differed only slightly from those of the precursor building blocks, the chemical shifts of the protons of the aromatic framework, the anthracene moiety and bridging ligands, were significantly shifted. Particularly diagnostic were the significant downfield shifts of the pyridyl signals ($\Delta\delta \sim 0.5$ ppm), associated with the loss in electron density upon coordination by the nitrogen lone pair to the platinum metal center. The signals from the "clip" (**4**) conversely shifted upfield, a result consistent with a transfer of electron density from the electron-rich bridging ligands to cationic **4**. Also noteworthy was that the α and β pyridyl protons of the bridging ligands, equivalent in free 4,4′-bpy, became inequivalent when incorporated into the assembled structure. This spectral feature is a manifestation of the restricted rotation of platinum−pyridine bonds.[20] Because the minimum for the energy barrier lies essentially perpendicular to the coordination plane of the platinum complex, and adjacent pyridyl groups are situated in a unique edge-to-edge arrangement rather than co-facially, the pyridyl protons pointed toward the inside of the macrocycles experience an environment different from those on the periphery. Specific proton assignments for the inner and outer pyridyl protons in **5** were established by NOESY NMR.[9c]

Support for the structure of **6** was provided by fast atom bombardment mass spectrometry (FABMS). Analysis of the hexafluorophosphate salt of **6** gave M − PF_6 and M − $2PF_6$ peaks at *m*/*z* 2878.1 and *m*/*z* 2733.9, respectively. Each ion was observed as a +1 charge state (i.e., separation of peaks by 1 *m*/*z* unit). The former was attributed to a loss of one PF_6 anion from a total of four, while the latter resulted from the loss of two PF_6 anions accompanied by the gain of one electron,

(19) Ellis, W. W.; Schmitz, M.; Arif, A. M.; Stang, P. J. *Inorg. Chem.* **2000**, *39*, 2547.

(20) (a) Davies, M. S.; Diakos, C. I.; Messerle, B. A.; Hambley, T. W. *Inorg. Chem.* **2001**, *40*, 3048. (b) Fuss, M.; Siehl, H.-U.; Olenyuk, B.; Stang, P. J. *Organometallics* **1999**, *18*, 758. (c) Stang, P. J.; Olenyuk, B. O.; Arif, A. M. *Organometallics* **1995**, *14*, 5281. (d) Brown, J. M.; Pérez-Torrente, J. J.; Alcock, N. W. *Organometallics* **1995**, *14*, 1195. (e) Alcock, N. W.; Brown, J. M.; Pérez-Torrente, J. J. *Tetrahedron Lett.* **1992**, *33*, 389.

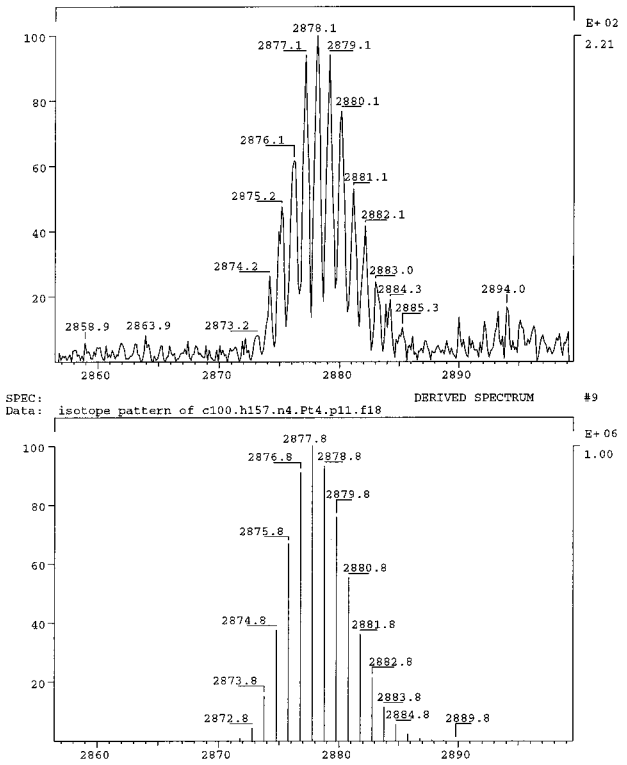

Figure 2. Experimental (top) and calculated (bottom) isotopic distribution pattern of M − PF_6 for **6**.

presumably from the support matrix. Also indicative of the proposed molecule was that the isotopic distribution patterns matched the calculated compositions. The calculated and experimental isotope distribution patterns of the M − PF_6 peak of **6** are shown in Figure 2.

The structures of both macrocycles **7** and **8** were unambiguously determined by X-ray crystallography. Quality single crystals of the perchlorate salt of **7** grew after several days at ambient temperature by vapor diffusion of diethyl ether into a concentrated DMF solution of the complex. The crystal lattice of **7** consists of well-separated, but electrostatically interacting, anions and rectangular cations. The asymmetric unit cell of **7** contains a half rectangle and two ClO_4 anions. The entire molecular rectangle is generated via an inversion center that is located at the midpoint of the two central bisethynylbenzene rings. One ClO_4 anion is crystallographically disordered. The structure refinement of **7** was thus based on a model including such a disordered anion and converged at $R = 0.081$ and $R_w = 0.215$. Otherwise, the ClO_4 anions appear to have a normal structure and warrant no further comments. The crystal packing is such that the cationic molecular rectangles lie parallel with each other approximately along the crystallographic {011} direction. All the ClO_4 anions are situated outside the rectangles in the pockets created by the triethylphosphine ligands from the different rectangles. The crystal structure of **7** is shown in Figure 3. The distortion in the molecular "clip" (**4**) affects the topology of **7** such that the BPEB bridging ligands are forced to bend slightly outward, which in turn causes the rectangle to appear bowed in the middle. This bending is accommodated primarily by the acetylenic moieties of the ligands. The overall dimensions of **7** give a more precise description of the overall topology. The approximate length of the rectangle is 30 Å. The height, as defined by the metals, is 5.7 Å, while the distance between the centroids of the central benzene rings of the BPEB ligand is 8 Å. As expected, the pyridyls were found perpendicular to the coordination planes of the platinum metals.

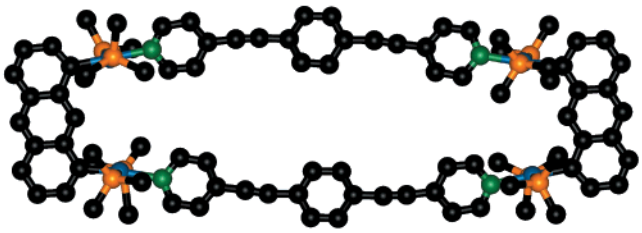

Figure 3. Ball and stick representation of the X-ray structure of **7**. Hydrogens, counterions, and the methyl groups from the triethylphosphines omitted for clarity. Colors: C, black; N, green; P, orange; Pt, blue.

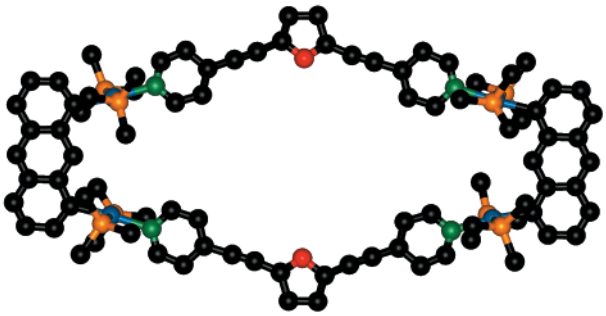

Figure 4. Ball and stick representation of the X-ray structure of **8**. Hydrogens, counterions, and the methyl groups from the triethylphosphines are omitted. Colors: C, black; O, red; N, green; P, orange; Pt, blue.

Interestingly, the central benzene ring of the ligand was also found to be coplanar with the rest of the aromatic framework. Although, at ambient temperature, the pyridyl signals are inequivalent because of restricted rotation, the ^1H NMR resonance from this central ring is a sharp singlet, indicating free rotation. A low-temperature NMR study was conducted on **7** in CD_2Cl_2. However, no significant broadening of this aromatic signal was detected as low as −80 °C, indicating continuous free rotation even at low temperatures. Despite having no apparent conformational preferences,[21] **7** showed no affinity toward neutral aromatic guests in organic solvents or acetone/water. Evidently, with no hydrophobic effect at work, there is not a driving force significant enough for the uptake of neutral guest molecules.[22]

Crystals of the hexafluorophosphate salt of **8** were grown in a manner analogous to those of **7**. Similarly, the crystal lattice of **8** consists of well-separated, but electrostatically interacting, anions and rectangular cations. The asymmetric unit cell of **8** also contains only a half rectangle and two PF_6 anions, one of which is slightly disordered. The entire rectangle is generated via an inversion center. In the crystal lattice, the parallel-packed molecular rectangles run approximately along the crystallographic {101} direction. The anions are found outside the rectangles in the area surrounded by the phosphine ligands. The impetus behind the synthesis of **8** was an attempt to test the limits for the ligand bite angle in this self-assembly motif. The free ligand (BPEF, Scheme 2) in this experiment is known[19] from X-ray analysis to possess a bite angle of approximately 127°. The crystal structure of **8** (Figure 4) shows that the bridging ligand is forced to bend inward, the opposite direction

(21) Phenylacetylenes naturally possess small rotational barriers (~0.6 kcal/mol) due to electronic factors. See: Young, J. K.; Moore, J. S. Acetylenes in Nanostructures. In *Modern Acetylene Chemistry*; Stang, P. J., Diederich, F., Eds.; VCH: New York, 1995.

(22) (a) Fujita, M.; Umemoto, K.; Yoshizawa, M.; Fujita, N.; Kusukawa, T.; Biradha, K. *Chem. Commun.* **2001**, 509. (b) Fujita, M. *Acc. Chem. Res.* **1999**, *32*, 53.

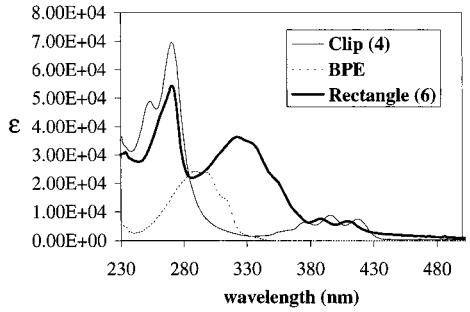

Figure 5. Absorption spectra for the molecular "clip" (**4**) (12.5 μM), BPE (12.5 μM), and molecular rectangle **6** (6.25 μM).

from the bridging 180° ligand in **7**. Additionally, an outward distortion of the Pt−N bonds appears to be a result of the ligand "pulling" the Pt atoms further apart; a distance of 5.9 Å as compared to a Pt−Pt distance of 5.6 Å in **4**. Because attempts at self-assembly reactions with more rigid 120° bridging ligands (containing no acetylenes) were unsuccessful, we judge that 130° must effectively be the lower limit for the angle that bridging ligands can have for this series of ring structures. For comparison purposes, in a recent paper by Sun and Lees,[6e] it was found that reaction of $Re(CO)_5Cl$, with a set of four ligands similar to those used in this study, resulted in squares, triangles, or dimers, depending on the specific ligand geometry. The apparent preference for smaller, strained systems over structures incorporating a larger number of subunits signifies the dominance of the entropy term over the enthalpy term and concurs with the greater structural flexibility of the subunit **4** relative to a simple metal atom. Admittedly, the topology of **8** is arguably not a rectangle because of its nonlinear linkage. However, this connectivity demands that the furanyl oxygen atoms always point directly toward the cavity, offering potential for novel types of host−guest interactions, because close inspection reveals that **8** is unique; it is cationic yet possesses hydrogen-bond acceptors within its cavity. The overall dimensions of this structure are about 28 Å in length, with a distance of 12.5 Å separating the centroids of the furanyl rings. This approximately gives a 1 nm × 1 nm cavity, but because of the offset arrangement in the crystal packing, channels were not formed.

Photophysical Properties. As previously noted, upon formation, molecular rectangles **5**−**8** all assume a characteristically intense orange color. As a representative example, the absorption spectrum of **6** is presented in Figure 5. The absorbance in the electronic spectrum exhibits near-UV transitions, which are red-shifted relative to BPE ($\pi-\pi^*$) and slightly blue-shifted relative to **4**. The extinction coefficient per BPE unit increases significantly upon rectangle formation, while the anthracene-based absorbance centered around 270 nm decreases, attributable to electronic reorganization for the conjugated, aromatic framework. Although anthracenes are widely applied as luminescent tags,[23] none was detected for these complexes, in accord with the assumption that the heavy-atom effect is the major contributor to fluorescence quenching.[24]

Mechanistic Studies. An intriguing prospect for self-assembly is that of enhancing the stability and/or potential utility of a thermodynamically assembled structure by rendering the kinetically labile interactions irreversible, that is, "locking" the structure in place once it is formed. Indeed, Fujita[25] has shown that a kinetically inert metal−ligand system becomes labile under the rigors of heat and excess salt. The assemblies then become "locked" by removal of the stimuli, i.e., cooling and salt removal. More recently, Raymond[26] demonstrated how a racemic mixture of tetrametallic homoconfigurational metal clusters ($\Delta\Delta\Delta\Delta$ and $\Lambda\Lambda\Lambda\Lambda$) could be resolved into an enantiopure form by the inclusion of a chiral guest molecule. The separated enantiomers were found to be remarkably stable toward racemization because of a high barrier for interconversion. Here, we demonstrate how postmodification[27] in the form of counterion exchange results in a stabilizing effect for these self-assembled structures (**5**−**8**).

In the early stages of this work, it was determined that organic solvents, such as methylene chloride, nitromethane, and pure acetone, were ineffective for self-assembly using **4**. The thermodynamic stabilization of rectangular metallacycles **5**−**8** was realized by the use of acetone/water mixtures, consistent with more polar media favoring the formation of charged species. Slow, partial evaporation of the acetone from the acetone/water solutions left orange crystals of the nitrate salts behind. However, several attempts at obtaining X-ray data from these crystals were unsuccessful because of their solvent dependent nature. As was expected, redissolving the crystals in the correct acetone-d_6/D_2O ratio regained the spectrum of the intact assemblies. On the other hand, dissolving these nitrate salt crystals in CD_2Cl_2 and monitoring their $^{31}P\{^1H\}$ and ^1H NMR spectra showed that the assemblies break apart by reverting into equilibrium mixtures within a few hours (Scheme 3). Thus, strong evidence is provided that these structures are true thermodynamic products, formed by way of equilibrium processes.

After self-assembly in acetone-d_6/D_2O was judged to be complete by NMR, the product was quantitatively precipitated out of solution as its PF_6 salt by the addition of excess KPF_6. The product was then simply collected on a frit, washed with excess water, and dried. Following anion exchange with weakly nucleophilic counterions (e.g., PF_6, BF_4, ClO_4, etc.), it was observed that the macrocycles do not fall apart when dissolved in CD_2Cl_2 (Scheme 3). The postmodified assembly **5** was periodically monitored by NMR and was found to remain intact in solution for nearly one year without decomposition. Enhanced stability was also observed for rectangles **6**, **7**, and **8**, but these eventually decomposed after a few months. A similar trend in stability was verified for the series **5**−**8** when their stability toward the coordinating solvent acetonitrile was tested. It was found that rectangle **5** is stable in CD_3CN, whereas **6**, **7**, and **8** are unstable toward solvolysis, breaking apart after 1−3 weeks. The relative stability for the series of structures was therefore determined to be **5** ≫ **8** ≈ **6** > **7**.

Considering that the vast majority of square planar substitution reactions are thought to occur by associative mechanisms,[28] the nitrate ion could possibly be playing the role of a nucleophile in the self-assembly. Hence, we describe this counterion effect as a type of kinetic stabilization. To further test this hypothesis, we carried out a reaction between the "clip" (**4**) and BPE (10^{-3} M) in a methylene chloride solution saturated with NH_4PF_6 (Scheme 4). The idea was that as nitrate gets displaced from

(23) De Silva, A. P.; Gunaratne, H. Q. N.; Gunnlaugsson, T.; Huxley, A. J. M.; McCoy, C. P.; Rademacher, J. T.; Rice, T. E. *Chem. Rev.* **1997**, *97*, 1515.

(24) Klessinger, M.; Michl, J. *Excited States and Photochemistry of Organic Molecules*; VCH: New York, 1995.

(25) Fujita, M.; Ibukuro, F.; Yamaguchi, K.; Ogura, K. *J. Am. Chem. Soc.* **1995**, *117*, 4175.

(26) Terpin, A. J.; Ziegler, M.; Johnson, D. W.; Raymond, K. N. *Angew. Chem., Int. Ed. Engl.* **2001**, *40*, 157.

(27) Lindsey, J. S. *New J. Chem.* **1991**, *15*, 153 and references therein.

(28) (a) Cross, R. J. *Adv. Inorg. Chem.* **1989**, *34*, 219. (b) Van Edlik, R.; Palmer, D. A.; Kelm, H. *Inorg. Chem.* **1979**, *18*, 572.

Scheme 3

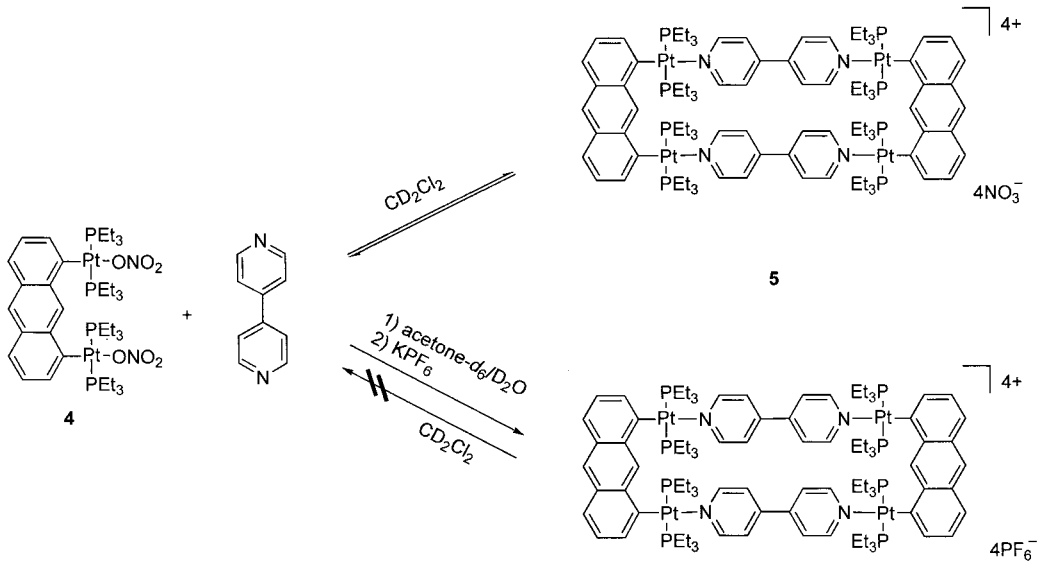

Scheme 4

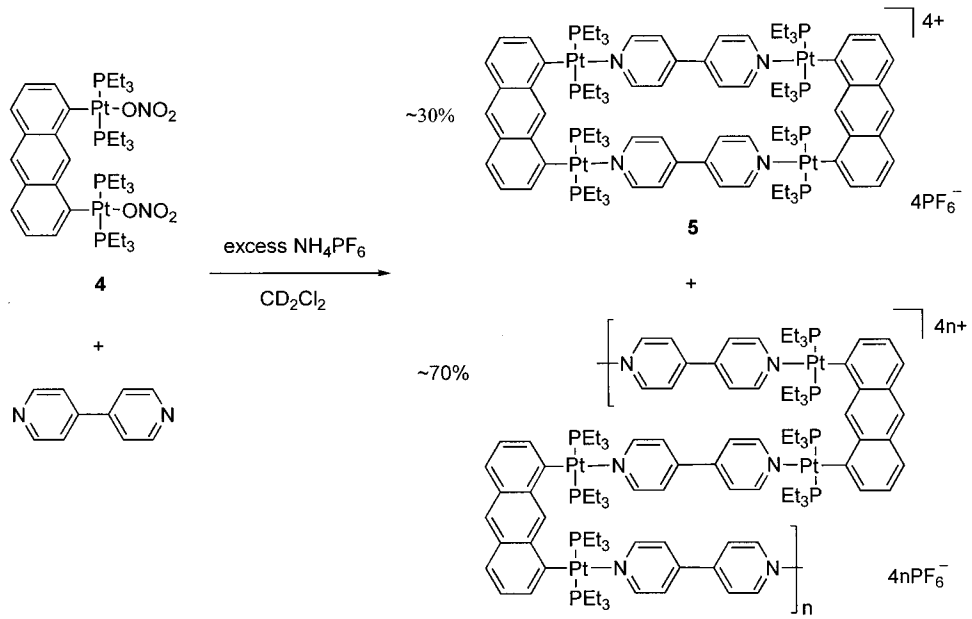

the metal center by pyridine, the uncoordinated nitrate will immediately be exchanged with PF_6 driven by the large excess, and only the forward reaction will be allowed to proceed, that is, no self-correction. As assessed by NMR, these reaction conditions led to the predominant formation of oligomeric material with ~30% of **5** formed. Consistent with macrocycle formation under kinetic control, running the same reaction at progressively lower concentrations increased the yield of rectangle **5**.

Conclusion

Nanoscopic metallacyclic rectangles (**5**−**8**) were prepared via modular self-assembly through the use of a molecular "clip" as a preconstructed shape-defining unit (**4**). FAB mass spectral data and X-ray crystallography unambiguously established their structure, which showed that the lengths of the rectangles range from 2 to 3 nm. Mechanistic studies show that the assembled structures can be locked in place by exchanging the nitrates with nonnucleophilic counteranions. While further studies are needed to firmly establish to what extent anions participate in self-assembly, the simple fact that the choice of counterion does have such an effect on structural stability offers valuable new insight. This postmodification method of stabilization endows the structures with newly found robust qualities and allows for greater flexibility in their study and application. For example, variable temperature NMR experiments can now be performed in a wide range of solvents chosen on the basis of boiling point, melting point, coordination ability, solubilizing properties, etc. Similar versatility is accessible for crystal growth experiments, cyclic voltametry, mass spectrometry, and new types of host−guest chemistry. These and related experiments are underway and will be the subjects of forthcoming reports.

Experimental Section

General Methods. 1,8-Dichloroanthraquinone was purchased from Aldrich. 1,8-Dichloroanthracene was prepared according to the known procedure.[15] The bridging ligand *trans*-1,2-bispyridylethylene (BPE) was purchased from Aldrich and sublimed prior to use. The other two ligands used in this study, 1,4-bis(4-ethynylpyridyl)benzene) (BPEB)[18] and 2,5-bis(4-ethynylpyridyl)furan (BPEF),[19] were synthesized by

published methods. NMR spectra were recorded on a Varian XL-300 or a Unity 300 spectrometer. Deuterated solvents were used as received. Proton chemical shifts are reported relative to residual protons of deuterated acetone (δ 2.05). ^{31}P $\{^1$H$\}$ chemical shifts (δ) are reported relative to an unlocked, external sample of H_3PO_4 (0.0 ppm). UV−vis spectra were recorded on a Hewlett-Packard 8452A spectrophotometer. Elemental analyses were performed by Atlantic Microlab, Norcross, Georgia. Melting points are uncorrected. The mass spectrum of **6** was obtained with a Finnigan MAT 95 mass spectrometer with a Finnigan MAT ICIS II operating system under positive fast atom bombardment (FAB) conditions. 3-Nitrobenzyl alcohol was used as a matrix in CH_2Cl_2 as a solvent, and polypropylene glycol and cesium iodide were used as a reference for peak matching.

X-ray Data Collection, Structure Solution, and Refinement. A single crystal of either **7** or **8** was selected from the reaction product and mounted on a thin glass fiber using silicone grease. The data were collected at −100 °C using a narrow frame method with scan widths of 0.3° in ω and exposure times of 20 s. A hemisphere of intensity data was collected in 1081 frames with the crystal-to-detector distance of 50.4 mm, which corresponds to a maximum 2θ value of 54.1°. Frames were integrated with the Bruker SAINT program. A semiempirical absorption correction based upon simulated ψ-scans was applied to the data set. Both structures were solved by a combination of direct methods and difference Fourier methods and refined with full-matrix least squares techniques. All the non-hydrogen atoms were refined anisotropically. The positions of the hydrogen atoms were calculated but not refined. Details of the data collection, structure solution, and refinement are given in Table 1.

1,8-Bis(*trans*-Pt(PEt$_3$)$_2$Cl)anthracene (3). To a stirred solution of $Pt(PEt_3)_4$ (2.3 g, 3.4 mmol) in freshly distilled toluene (60 mL) under argon was added, in portions, 1,8-dichloroanthracene (336 mg, 1.36 mmol). The resulting bright red solution was then maintained for 3 days in an oil bath at 105−110 °C. The solvent was removed in vacuo at 40 °C, and the residue, now in open air, was suspended in methanol (15 mL) and gently refluxed for 45 min. The suspension was then allowed to cool and the product collected on a frit and washed twice with cold methanol (5 mL each) to give **1** as a yellow solid. A 1.3 g quantity (86% yield) was obtained. Mp 262−268 °C (dec). ^{1}H NMR (CD_2Cl_2, 300 MHz): δ 9.33 (s, 1H, H_9), 8.15 (s, 1H, H_{10}), 7.56 (m, 4H, $H_{2,4,5,7}$), 6.98 (m, 2H, $H_{3,6}$), 1.67 (m, 24H, PCH_2CH$_3$), 0.93 (m, 36H, PCH$_2$CH_3). ^{31}P$\{^1$H$\}$ NMR (CD_2Cl_2, 121.4 MHz): δ 10.7 (s, $^1J_{PPt}$ = 2756 Hz). ^{13}C$\{^1$H$\}$ NMR (CD_2Cl_2, 125.7 MHz): δ 142.3 (m, $^1J_{CPt}$ = 973 Hz, C$_i$−Pt), 138.9, 135.8, 133.2, 131.9, 126.3, 125.8, 122.0, 14.8 (m, PCH$_2$CH$_3$), 8.3 (s, PCH$_2$CH$_3$). Anal. Calcd for $C_{38}H_{68}Cl_2P_4Pt_2$: C, 41.12; H, 6.18. Found: C, 41.19; H, 6.24.

1,8-Bis(*trans*-Pt(PEt$_3$)$_2$(NO$_3$))anthracene (4). To a stirred solution of 1,8-bis(*trans*-Pt(PEt$_3$)$_2$Cl)anthracene (500 mg, 0.450 mmol) in acetone (60 mL) was added, all at once, silver nitrate (153 mg, 0.900 mmol). The reaction was stirred for 3 h in the dark, after which the reaction mixture was filtered through a bed of Celite and the filtrate evaporated to dryness under reduced pressure. The crude yellow solid was then suspended in 20 mL of water and sonicated for 15 min. The suspension was then filtered, washed with excess water, and air-dried. Next, on a steam bath, the product was taken up in a minimum amount of boiling methanol, filtered hot, and placed in the freezer for 1−2 days. The yellow crystals that formed were collected on a frit and dried in vacuo to give 430 mg (83% yield) of analytically pure product. Mp 257−258 °C (dec). ^{1}H NMR (acetone-d_6, 300 MHz): δ 9.54 (s, 1H, H_9), 8.24 (s, 1H, H_{10}), 7.67 (m, 4H, $H_{2,4,5,7}$), 7.05 (m, 2H, $H_{3,6}$), 1.63 (m, 24H, PCH_2CH$_3$), 1.03 (m, 36H, PCH$_2$CH_3). ^{31}P$\{^1$H$\}$ NMR (acetone-d_6, 121.4 MHz): δ 14.6 (s, $^1J_{PPt}$ = 2855 Hz). ^{13}C$\{^1$H$\}$ NMR (acetone-d_6, 125.7 MHz): δ 138.4, 133.4, 132.6, 130.1, 127.6, 127.5, 125.9, 123.5, 15.3 (m, PCH$_2$CH$_3$), 8.0 (s, PCH$_2$CH$_3$). UV−vis (CH_2Cl_2) λ_{max} (ϵ) [nm (cm^{-1} M^{-1})] 254 (49 200), 270 (69 700), 376 (7400), 396 (9200), 418 (8600). Anal. Calcd for $C_{38}H_{68}N_2O_6P_4Pt_2$: C, 39.24; H, 5.89; N, 2.41. Found: C, 39.50; H, 5.92; N, 2.38.

General Procedure for the Preparation of Compounds 5−8. In a 2 dram vial equipped with a magnetic stir bar were placed solid 1,8-bis(*trans*-Pt(PEt$_3$)$_2$(NO$_3$))anthracene (20.0 mg, 0.0172 mmol) and an equimolar amount of the appropriate bridging ligand. Next, 0.5 mL of acetone-d_6 and 0.5 mL of D_2O were added to the vial, which was then sealed with Teflon tape and heated in an oil bath at 50−55 °C, with stirring. After 10−15 h, the initial pale yellow suspension gradually turned bright orange and became homogeneous. The orange solution was then transferred to an NMR tube for analysis. The product was precipitated with KPF_6, collected on a frit, washed with excess water, and dried in vacuo. Note: Samples for elemental analysis were obtained by allowing the original acetone/water solution to slowly evaporate.

Cyclobis[(1,8-bis(*trans*-Pt(PEt$_3$)$_2$(NO$_3$))anthracene)(4,4′-dipyridyl)] (5). ^{1}H NMR (acetone-d_6/D_2O, 300 MHz): δ 9.60 (s, 2H, H_9), 9.28 (d, 4H, $^3J_{HH}$ = 6.3 Hz, H_α-Py), 9.22 (d, 4H, $^3J_{HH}$ = 5.7 Hz, H_α-Py), 8.88 (d, 4H, $^3J_{HH}$ = 6.0 Hz, H_β-Py), 8.63 (d, 4H, $^3J_{HH}$ = 6.3 Hz, H_β-Py), 8.43 (s, 2H, H_{10}), 7.77 (d, 4H, $^3J_{HH}$ = 8.4 Hz, $H_{4,5}$), 7.70 (d, 4H, $^3J_{HH}$ = 6.9 Hz, $H_{2,7}$), 7.20 (m, 4H, $H_{3,6}$), 1.54 (m, 48H, PCH_2-CH$_3$), 0.88 (m, 72H, PCH$_2$CH_3). ^{31}P$\{^1$H$\}$ NMR (acetone-d_6/D_2O, 121.4 MHz): δ 8.6 (s, $^1J_{PPt}$ = 2647 Hz). UV−vis (CH_2Cl_2) λ_{max} (ϵ) [nm (cm^{-1} M^{-1})] 272 (53 500), 324 (3 6 100), 336 (33 300), 390 (7500), 412 (6600). Anal. Calcd for $C_{96}H_{152}N_8O_{12}P_8Pt_4$·8$H_2O$: C, 41.44; H, 6.09; N, 4.03. Found: C, 41.43; H, 5.92; N, 4.05.

Cyclobis[(1,8-bis(*trans*-Pt(PEt$_3$)$_2$(NO$_3$))anthracene)(1,2-bispyridylethylene)] (6). ^{1}H NMR (acetone-d_6/D_2O, 300 MHz): δ 9.51 (s, 2H, H_9), 8.98 (m, 8H, H_α-Py), 8.33 (s, 2H, H_{10}), 8.19 (m, 8H, H_β-Py), 7.98 (s, 4H, H_{alkene}), 7.69 (d, 4H, $^3J_{HH}$ = 8.1 Hz, $H_{4,5}$), 7.63 (d, 4H, $^3J_{HH}$ = 6.6 Hz, $H_{2,7}$), 7.15 (m, 4H, $H_{3,6}$), 1.44 (m, 48H, PCH_2CH$_3$), 0.81 (m, 72H, PCH$_2$CH_3). ^{31}P$\{^1$H$\}$ NMR (acetone-d_6/D_2O, 121.4 MHz): δ 8.4 (s, $^1J_{PPt}$ = 2644 Hz). UV−vis (CH_2Cl_2) λ_{max} (ϵ) [nm (cm^{-1} M^{-1})] 272 (53 500), 324 (36 100), 336 (33 300), 390 (7500), 412 (6600). Anal. Calcd for $C_{100}H_{156}N_8O_{12}P_8Pt_4$: C, 44.64; H, 5.84; N, 4.16. Found: C, 44.43; H, 5.90; N, 4.11.

Cyclobis[(1,8-bis(*trans*-Pt(PEt$_3$)$_2$(NO$_3$))anthracene)(1,4-bis(4-ethynylpyridyl)benzene)] (7). ^{1}H NMR (acetone-d_6/D_2O, 300 MHz): δ 9.45 (s, 2H, H_9), 9.05 (d, 4H, $^3J_{HH}$ = 5.4 Hz, H_α-Py), 8.96 (d, 4H, $^3J_{HH}$ = 6.3 Hz, H_α-Py), 8.36 (s, 2H, H_{10}), 8.05 (d, 8H, $^3J_{HH}$ = 6.3 Hz, H_β-Py), 7.76 (s, 8H, $H_{phenylene}$), 7.71 (d, 4H, $^3J_{HH}$ = 8.1 Hz, $H_{4,5}$), 7.64 (d, 4H, $^3J_{HH}$ = 6.6 Hz, $H_{2,7}$), 7.16 (m, 4H, $H_{3,6}$), 1.44 (m, 48H, PCH_2-CH$_3$), 0.82 (m, 72H, PCH$_2$CH_3). ^{31}P$\{^1$H$\}$ NMR (acetone-d_6/D_2O, 121.4 MHz): δ 8.4 (s, $^1J_{PPt}$ = 2643 Hz). UV−vis (CH_2Cl_2) λ_{max} (ϵ) [nm (cm^{-1} M^{-1})] 272 (68 000), 350 (65 100), 370 (54 700), 410 (10 200). Anal. Calcd for $C_{116}H_{160}N_8O_{12}P_8Pt_4$·8$H_2O$: C, 45.97; H, 5.85; N, 3.70. Found: C, 46.38; H, 5.76; N, 3.53.

Cyclobis[(1,8-bis(*trans*-Pt(PEt$_3$)$_2$(NO$_3$))anthracene)(2,5-bis(4-ethynylpyridyl)furan)] (8). ^{1}H NMR (acetone-d_6/D_2O, 300 MHz): δ 9.23 (s, 2H, H_9), 9.07 (d, 4H, $^3J_{HH}$ = 4.8 Hz, H_α-Py), 8.90 (d, 4H, $^1J_{HH}$ = 5.7 Hz, H_α-Py), 8.34 (s, 2H, H_{10}), 8.00 (m, 8H, H_β-Py), 7.70 (m, 4H, $H_{2,4,5,7}$), 7.20 (s, 4H, $H_{furanyl}$), 7.15 (m, 4H, $H_{3,6}$), 1.41 (m, 48H, PCH_2CH$_3$), 0.85 (m, 72H, PCH$_2$CH_3). ^{31}P$\{^1$H$\}$ NMR (acetone-d_6/D_2O, 121.4 MHz): δ 8.7 (s, $^1J_{PPt}$ = 2644 Hz). UV−vis (CH_2Cl_2) λ_{max} (ϵ) [nm (cm^{-1} M^{-1})] 272 (31 300), 380 (39 600), 402 (36 500). Anal. Calcd for $C_{112}H_{156}N_8O_{14}P_8Pt_4$: C, 46.93; H, 5.49; N, 3.91. Found: C, 46.67; H, 5.55; N, 3.76.

Acknowledgment. Financial support by the National Science Foundation (CHE-9818472) and the National Institutes of Health (GM-57052) is gratefully acknowledged. We thank Dr. Atta Arif for the solution of the crystal structure of **4** and Dr. Elliot Rachlin for obtaining the mass spectral data for **6**.

Supporting Information Available: Tables of crystal data, structure refinement details, and SHELXL file for compounds **4**, **7**, and **8** (pdf). This material is available free of charge via the Internet at http://pubs.acs.org.

JA0114355